Modeling of protein electrophoresis in silica colloidal crystals having brush layers of polyacrylamide

Robert E. Birdsall, **Brooke M. Koshel**, **Yimin Hua**, **Saliya N. Ratnayaka**, and **Mary J. Wirth**[*]
Department of chemistry, 560 Oval Drive, Purdue University, West Lafayette, IN 47907

Abstract

Sieving of proteins in silica colloidal crystals of mm dimensions is characterized for particle diameters of nominally 350 and 500 nm, where the colloidal crystals are chemically modified with a brush layer of polyacrylamide. A model is developed that relates the reduced electrophoretic mobility to the experimentally measurable porosity. The model fits the data with no adjustable parameters for the case of silica colloidal crystals packed in capillaries, for which independent measurements of the pore radii were made from flow data. The model also fits the data for electrophoresis in a highly ordered colloidal crystal formed in a channel, where the unknown pore radius was used as a fitting parameter. Plate heights as small as 0.4 μm point to the potential for miniaturized separations. Band broadening increases as the pore radius approaches the protein radius, indicating that the main contribution to broadening is the spatial heterogeneity of the pore radius. The results quantitatively support the notion that sieving occurs for proteins in silica colloidal crystals, and facilitate design of new separations that would benefit from miniaturization.

1 Introduction

Size-based separations of proteins are often used as one of the dimensions of separation in proteomics [1], where the ease of coupling to another separation dimension or to mass spectrometry is critical. Size-based separations of proteins are widely used in the pharmaceutical industry, where there is an urgent need for high throughput methods in the development of formulations because significant aggregation occurs at therapeutic concentrations [2]. Protein size-based analyses have often employed slab gel electrophoresis, which has the ability to run samples in parallel with good resolution [3]. However, slab gel separations are slow and laborious [4], and difficult to automate [5]. Capillary electrophoresis enables high throughput by its ease of automation [6], and previous work demonstrated that polyacrylamide gels cast in narrow capillaries could separate proteins and peptides [7], as well as ssDNA fragments [8], giving improved efficiency through better heat dissipation [7]. Mechanical instability and bubble formation lead to the use of linear polymer solutions, which avoided these problems [9]. While these are useful for single-strand DNA separations, they are less useful for proteins because the contamination by the polymer solution prevents the use of mass spectrometry without an additional separation step. A sieving medium for proteins is needed that combines the advantages of capillaries and gels to allow automation without having the sieving medium elute.

A new approach is to create a rigid porous network with colloidal silica, which forms face-centered cubic crystals in thin channels [10] and in capillaries [11]. The solid matrix gives

[*]mwirth@purdue.edu.

high thermal conductivity to reduce broadening due to heating [12]. Work by Zeng *et al.* was the first to demonstrate that sieving of proteins and DNA fragments occurs in silica colloidal crystals [10]. They subsequently used this medium to continuously fractionate double-strand DNA based on size, from 7 to 100 kbp[13]. The size-based separations were achieved over lengths on the mm scale, and such miniaturization raises the possibility of preparing densely packed parallel devices for high throughput in size-based measurements of proteins. Presently, there is no model for sieving in silica colloidal crystals, and a model would facilitate the design of new devices.

The objective of this study is to develop a model of protein sieving through silica colloidal crystals, and to validate this model experimentally. The silica surfaces are chemically modified with a brush layer of polyacrylamide to avoid protein adsorption and electro-osmotic flow. Silica particles are packed in capillaries to allow the direct measurement of porosity [14], which is advantageous for testing the model. The applicability of the model to silica colloidal crystals packed in channels on planar substrates is also studied.

2 Materials and methods

2.1 Materials

Particles of nominally 350 and 500 nm in diameter were purchased from NanoGIANT LLC (Scottsdale, AZ). After calcining for 12 hr at 600 °C, the average diameters were determined by SEM to be 339 ± 3 nm and 483 ± 5 nm, respectively. These will be referred to by their nominal sizes, whereas the measured sizes were used in all calculations. Proteins, solvents, reagents, buffers and other supplies were purchased from commercial sources, and these are detailed in the Supporting Information. The ligand tris (2-dimethylaminoethyl) amine was synthesized as previously described by Xiao *et al.* [15].

2.2 Capillary preparation

Capillaries were conditioned using a syringe pump (Harvard Apparatus Holliston, MA). A 0.1 M HNO_3 solution was pumped through the capillary at a rate of 100 μl/min for ten minutes, followed by ultrapure water, and 200% ethanol for 10 and 20 min, respectively. The capillaries were dried under vacuum for 45 min at 80 °C. Silica slurries were prepared at a 30 % (w/w) concentration in water and sonicated in a water bath. Slurries were wicked into capillaries of 12 cm in length, and then packed under pressure at 345 bar with sonication for 15 min using a 0.5 μm frit. After packing, the frit was removed and the capillary was allowed to dry in a dessicator. Packing lengths on the order of 2 cm were used for the flow and electrophoresis measurements.

The packed capillaries were modified with polyacrylamide, as detailed previously [12, 15]. Briefly, the silica surface was silylated with initiator, and linear polyacrylamide chains were grown using a complex of CuCl with tris (2-dimethylaminoethyl) amine as the catalyst. The solution of acrylamide monomer and CuCl catalyst was wicked into the capillary and allowed to polymerize. The details of this atom transfer radical polymerization method are provided in the Supporting Information.

2.3 Channel preparation

The procedure previously described by Zeng et al. [10] was used to create highly ordered colloidal crystal in a channel using the 500 nm particles. Both glass and fused silica slides were chemically modified with 50 mM solution of n-butyldimethylchlorosilane in anhydrous toluene for 48 hrs under nitrogen. The slides were then rinsed with dry toluene and dried under vacuum at 80 °C. A 1-mm wide stripe of 1-cm in length was masked off on the fused silica slide, and chemically etched with an ammonium bifluoride salt paste for 1

hr. A chemically modified glass slide was used to cover the channel, and the assembly was secured using binder clips. A 10% (w/w) silica colloid was wicked into the channel, which was allowed to dry at room temperature for 48 hr. After drying, the cover glass slide was carefully removed and the packed channel was modified using the same polymerization reaction as for the capillary. The one difference is that the entire slide immersed in the reagent solution.

2.4 Protein preparation

Proteins were reconstituted in 500 µL of a phosphate buffered saline solution of pH 7.6 at a concentration of 2 mg/mL and then labeled with Alexa Fluor 546 fluorescent dye (Invitrogen Inc. Carlsbad, CA). Prior to use, labeled proteins were diluted to a concentration of 0.05 mg/ml and denatured at 80 °C for 5 min in a buffer (pH 8.0) containing 62 mM Tris, 1 mM EDTA, 3 % sucrose, and 2% SDS (hereafter called "denaturing buffer").

2.5 Porosity determination

Porosity measurements for capillaries were made by measuring volume flow rate at a series of known pressures. An Accela UHPLC Pump (Thermo Fisher Scientific, Waltham, MA) was attached to a tee split with a 50 µm bore (Vici, Houston, TX). One arm of the split was connected to the packed capillary of interest through a union using two stainless steel nut/ferrule combinations (Vici, Houston, TX) and the other arm was a waste capillary of 50 cm in length. The solvent of choice was pumped through the packed capillary until the pressure became static with a standard deviation of 0.3 bar. A 400-µm i.d. capillary sleeve was then used to collect the solvent flow out of the packed capillary for a set time. After solvent collection the capillary sleeve was removed and a digital image of the solvent plug in the sleeve was taken using a Nikon Zoom Stereomicroscope (Nikon Instruments Inc., Melville, NY) to determine the volume collected. Back pressure from the union and waste capillary was corrected by calibrating with an empty capillary set up in place of the packed capillary. The slight evaporation of the solvent was accounted for by using a calibration curve of volume versus time for a series of empty sleeves loaded with solvent.

2.6 Electrophoresis

For capillary experiments, dual reservoir PDMS holders were placed on a glass slide to prevent electrophoresis gas bubbles from entering the channel [11, 12]. The capillaries packed with 350 nm and 500 nm particles were saturated with a commonly used protein electrophoresis TGS running buffer composed of 25 mM tris, 192 mM glycine, 0.1% (w/v) SDS (pH 8.0) overnight, and electrically conditioned at 50 Vcm^{-1} using a high-voltage power supply (10A25A Series, Ultravolt, Ronkonkoma, NY) controlled by LabView until the current became static. Fluorescence labeled proteins were prepared at a concentration of 0.05 mg/mL in the denaturing buffer and loaded into the capillaries by diffusion for 1 s. The capillary was then mounted between the dual PDMS reservoirs in a tight fitting notch, with the protein loaded at the cathode end. Platinum electrodes were placed in the outer reservoir wells. The reservoirs were then filled with TGS running buffer, and an electric field of 50 Vcm^{-1} was applied as above. Experimental setup and the detection procedure using fluorescence microscopy, are detailed in the supporting information.

Open tube electrophoretic mobility, μ_0, was determined in triplicate with a 50.0 cm polyacrylamide coated CE capillary (Sepax Technologies, Inc., Newark, DE) using the same experimental setup as for electrophoresis in the packed capillaries. For this measurement, the labeled proteins were prepared individually in concentrations of 0.2 mg/ml and loaded into the capillary by diffusion for two seconds. The proteins were then electrophoretically migrated to a detection window set at 40.0 cm in length at 100 Vcm^{-1}.

Measurements on the packed channels were performed under similar conditions as the packed capillaries. Modified channels were wetted with the TGS running buffer and covered with a tight fitting PDMS seal at each end of the channel. The PDMS seal was fabricated using a (10:1) mixture of SYLGARD® 184 elastomer and curing agent. Pressure was used to hold the seal in place to ensure a tight fit against the surface of the channel to avoid drying, and electrical conditioning was performed in the same manner as previously described. Proteins were electro-kinetically loaded into the channel under 300 Vcm^{-1} for 30 s. After stacking, an electric field of 50 Vcm^{-1} was used for separation. Imaging and data treatment were the same as previously described for the capillaries.

3 Results and discussion

3.1 Theory

Understanding transport through gel was enabled by Ogston, who derived an exponential relationship between the fractional free volume, f, accessible to spherical analytes of radius, R, in a random network of infinitely long gel fibers with radius, r, of fiber concentration, C [16, 17].

$$f = \exp\left(-\frac{\pi}{4}(R+r)^2 \cdot C\right) \quad (1)$$

This model was extended to gel electrophoresis by Morris, who proposed that electrophoretic mobility, μ is decreased relative to its value in open solution, μ_0, by the accessible volume fraction, f [18].

$$\frac{\mu}{\mu_0} = f \quad (2)$$

Rodbard and Chrambach's refinement of the Ogston-Morris model for gel electrophoresis in the limiting case of long fibers led to the Ogston Morris Rodbard Chrambach (OMRC) equation, which is applicable to non-spherical molecules as well [19].

$$\frac{\mu}{\mu_0} = \exp\left(-c \cdot C \cdot (R+r)^2\right) \quad (3)$$

In this equation, c is a constant for the specified electrophoretic system, whereas the gel fiber concentration, C, is related to the amount of cross-linker, which controls the pore size. Once calibrated for c using protein standards, electrophoresis provides an estimate for molecular radius, and thereby molecular weight, in addition to separating proteins.

For describing electrophoresis in colloidal crystals, we start with Giddings' description of the fractional volume that is accessible within a cylindrical pore of radius, ξ, and a protein of radius, R [23, 24].

$$f_{pore} = \frac{(\xi - R)^2}{\xi^2} \quad (4)$$

This equation by itself would describe the medium as a network of cylindrical pores, but it is necessary to account for the fact that the pores themselves occupy only a fraction, ε, of the total volume of the medium. Therefore, the Giddings function must be scaled by ε. This is

analogous to multiplying the equilibrium constant by the ratio of the volumes of stationary and mobile phase to describe chromatographic retention.

$$\frac{\mu}{\mu_0}=f_{total}=\left(\varepsilon \cdot \frac{(\xi-R)^2}{\xi^2}\right) \quad (5)$$

Unlike the case for gels, this equation does not have an empirical constant. Both ε and ξ can be determined independently of electrophoresis measurements by using flow measurements through the packed capillaries. The porosity can be determined experimentally from the volume flow rate, F, before the reaction of acrylamide by using the Kozeny-Carman relation [14], given in Equation 6.

$$F=\frac{P}{\eta}\frac{\pi \cdot r_c^2 \cdot d_p^2}{180 \cdot L}\frac{\varepsilon^3}{(1-\varepsilon)^2} \quad (6)$$

To use equation 6, the flow rate is measured, and the known parameters of pressure, P, capillary radius, r_c, particle diameter, d_p, viscosity, η, and column length, L, are used to calculate porosity, ε. In this measurement, we use acetonitrile as the fluid because it is miscible with the silane modified surface. This ensures that the no-slip boundary condition is maintained, which is a necessity for applying equation 6

The value of ξ can be determined from flow measurements after the formation of the polyacrylamide layer, in this case using water as the fluid to hydrate the polymer layer as fully as it is hydrated during electrophoresis. A smaller porosity, ε_{hyd}, results from the hydrated chains, and is again determined by the Kozeny-Carman relationship.

$$F_{hyd}=\frac{P}{\eta}\frac{\pi \cdot r_c^2 \cdot d_p^2}{180 \cdot L}\frac{\varepsilon_{hyd}^3}{\left(1-\varepsilon_{hyd}\right)^2} \quad (7)$$

The concept behind this step in applying the model is depicted in Figure 1a, which shows that the hydrated polyacrylamide occupies some of the volume, thereby reducing the pore radius to ξ. The assumption that the proteins are excluded from the polyacrylamide layer is supported by earlier work [12, 26]. The water inside the polyacrylamide layer is thereby taken to behave as a stagnant layer that is porous only to water and other small molecules [25]. The notion that the fluid velocity goes to zero at the surface of the polyacrylamide layer is illustrated in Figure 1b.

Flow through packed beds of particles has been described by treating the packed bed as a set of parallel open tubes with fictive tube radius, r_{tube}, which is directly related to the resistance to flow [27, 28].

$$r_{tube}=\frac{d_p}{3} \cdot \frac{\varepsilon_{hyd}}{\left(1-\varepsilon_{hyd}\right)} \quad (8)$$

In reality, the tube radius undulates through the packed bed, hence r_{tube} is related to the root-mean-square cross-section. We approximate the pore radius in our model as this tube radius for the purpose of determining its value from independent measurement of flow, rather than determining it from fitting the electrophoresis data.

$$\xi = r_{tube} \quad (9)$$

These relationships provide the parameters to enable use of Equation 5 for describing the electrophoretic mobility of proteins in colloidal crystals.

3.2 Flow results

Porosity measurements for the capillaries were made by characterizing their resistance to flow. Figure 2 shows the plots of pressure vs. volume flow rate for capillaries packed with 350 and 500 nm particles. The pressure reached up to 600 bar and the flow rate reached up to 8 nL/min. The pressure is normalized by viscosity in these plots, and the small dependence of viscosity on pressure was accounted for [29]. The flow was measured first for the particles with the silane initiator monolayer prior to the ATRP modification using acetonitrile as the fluid. The data and each fit to the Kozeny-Carman equation are shown in Figure 2 There is a small negative intercept in each case, consistent with the observation that a small and consistent amount of fluid remained over the outside of the packed capillary rather than entering the receiving capillary. Since the information is in the slope, the slight negative intercept does not interfere with the determination of pore radius. The slopes appear to be similar on this scale for the two particles sizes modified only by the silanes, but in fact, they differ by ratio of particle diameters. The porosities of the colloidal crystals, ε, were determined from each fit to the Kozeny Carman equation to be 0.32($\pm$0.01) and 0.314($\pm$0.006), for the 350 nm and 500 nm particles, respectively. These porosity values are in good agreement with previous reports for packed capillaries, which showed polycrystalline morphology with small domains [30], explaining why the porosity is somewhat larger than the value of 0.26 for perfect face-centered cubic crystals. Flow measurement after the polyacrylamide layer was grown, using acetonitrile as the fluid, show no change in slope outside of the experimental uncertainty. This indicated that the retracted polymer chains in the presence of acetonitrile occupy a negligible fraction of the pore volume.

Figure 2 shows that when water was used as the fluid, the flow rate was significantly lower. This indicates that a significant fraction of the interstitial volume is occupied by the polyacrylamide layer as it becomes swelled by hydration. The new porosities are 0.130($\pm$0.007) and 0.143($\pm$0.005) for the 350 and 500 nm particles, respectively. These porosity values indicate that the swollen polyacrylamide chains take up approximately half of the pore volume. Using Equation 8, the pore radii, ξ, are calculated to be 17 and 27 nm for the 350 and 500 nm particles, respectively. We note that the measured particle diameters of 339 and 483 were used in each of these calculations. These results are summarized in Table 1, and they provide the parameters needed to describe the reduced mobilities for the model in equation 5.

Incidentally, one can use the data of Figure 2 to calculate the average thickness of the hydrated polyacrylamide layer. These calculated thicknesses are 36 nm and 47 nm for the 350 and 500 nm particles, respectively. A possible reason for the somewhat thinner layer for the 339 nm particles might be the steric restriction of the growing chain in the smaller pores. These thicknesses are more than tenfold larger than the calculated Debye layer thickness of 2.1 nm, based on the ionic strength of 20 mM for the running buffer. Consequently, the surface potential decreases by many orders of magnitude over this distance, therefore, electro-osmotic flow can be regarded as negligible.

3.3 Electrophoresis

Mobilities of four proteins were determined from replicate electropherograms for each of the two different capillaries, and these electropherograms are shown in Figures 3a and 3b. For these data, the peaks were detected as they electromigrated past a fixed separation distance of 4 mm. The reproducibility is good for both particle sizes. The data show that the smaller proteins are not baseline resolved, and that the resolution for the smaller proteins is better when using the smaller particles. The mobilities and their R.S.D. values are summarized in Table 1. Also included in Table 1 are the mobilities, μ_0, of the same proteins in an open capillary that was chemically modified with polyacrylamide. These values allow calculation of the reduced mobilities, μ/μ_0. The reduced mobilities are somewhat smaller for the smaller particles, which is qualitatively consistent with the smaller pore radius.

To test the model, the reduced mobilities are plotted vs. molecular weight for the experimental data in Figure 3c and 3d. The theoretical relationship, Equation 5, is plotted on the same graph using the experimentally determined porosity and pore radius, as detailed in the previous section. For the theoretical equation, the protein radius was related to molecular weight using Equation 10 from Narang et al., which relates radius of gyration to the number of amino acid units, N [31].

$$R=N^{\frac{3}{5}} \quad (10)$$

We use radius of gyration because Kopecka *et al.* had shown that electrophoretic mobility of ssDNA is best described when using R as the radius of gyration [22]. Figure 3c and 3d show that the model describes the data well for both particle sizes without any adjustable parameters. This indicates that the fictive pore radius from flow in a packed bed also applies to sieving in a packed bed.

It is interesting to explore whether the model introduced here describes protein sieving in more ordered media. We prepared a highly ordered crystal in a planar channel with 500 nm particles, and chemically modified it with polyacrylamide. An SEM image of a channel cross-section is provided in Figure S1 of the supporting Information to show the face-centered cubic crystallinity. Figure 4 shows a plot from a spatial image of the channel at one point in time, t= 150 s, which was the one instant when the reservoir and the four proteins spanned the entire field of view of the microscope. The plot shows that a good separation was achieved in this 2.5 mm separation length. It is noted that the order of peaks is backwards from the electropherograms in Figure 3 because the electropherogram in Figure 4 is plotted in distance units rather than time units. It was not feasible to use a fixed detection position because the mobilities are so much more disparate. Consequently, the mobilities were determined from measurements at multiple times and positions along the channel, and these averages are summarized in Table 1.

To fit the data to the model, it is assumed that the porosity is $\varepsilon = 0.26$, which applies to face-centered cubic crystals. Since ε_{hyd} cannot be determined independently due to the inability to make flow measurements, we use the pore radius as a fitting parameter. The reduced mobility data and the theoretical plot are shown in Figure 4b for the best-fit pore radius of 6 nm. Use of equation 8 allows the polyacrylamide thickness to be estimated, and the result is 45 nm. This is reasonable to expect because the channel had more access to polymerization reagents since it had been reacted by immersion in the monomer and catalyst solution. By contrast, the capillaries had been filled with a fixed amount of monomer and catalyst, and allowed to react. The narrower pores serve to show that the model applies to an ordered medium. Although it cannot be determined whether an empirical fitting parameter would be needed, it can be concluded that the model provides the right functional form.

These materials show promise for their potential in miniaturization. For the 350 nm particles packed in the capillary, the resolution for the lowest molecular weight proteins, lysozyme and trypsin inhibitor, is 0.87, which translates to an ability to resolve proteins differing by 6 kDa with unit resolution over the distance of 4 mm. Regarding efficiency, the lowest plate heights are seen for the smallest protein, lysozyme, where the plate height is 1.1 µm for the 350 nm particles and 0.4 µm for the 500 nm particles. These are outstanding for electrophoresis, but are more than ten-fold higher than the plate height for electrochromatography in a colloidal crystal [33]. The likely reason is spatial heterogeneity of the pore radius over the microscale to macroscale. As the pore radius approaches the size of the protein, i.e., $\xi \approx R$, small variations in pore radius will give large variations in reduced mobility, $\{(\xi-R)/\xi\}^2$. This interpretation is supported by the fact that the peaks are much broader for larger proteins and for smaller pores, a phenomenon that is especially obvious in the electropherogram of Figure 4. This leaves room for improving the materials for further miniaturizing separations.

4 Concluding remarks

The model provides the physical insight that the same average pore radius inside a packed bed that controls flow also controls sieving in electrophoresis. Without this insight, one might have thought that only the limiting pore diameter depicted in Figure 1a controls sieving. A more homogeneous medium to generate narrower peaks might be made by using smaller crystalline domains to avoid long excursions at domain boundaries. Already the mm lengths needed to separate proteins that differ by a factor of two in molecular weight points to the possibility of a high-throughput assay of formulated protein drugs with respect to aggregates. The model developed in this work can facilitate design of such applications.

Supplementary Material

Refer to Web version on PubMed Central for supplementary material.

Acknowledgments

Abbreviations

SDS	sodium dodecylsulfate
TGS	tris, glycine, and SDS
PDMS	polydimethylsiloxane
PAAm	polyacrylamide
RSD	relative standard deviation

References

1. Fang XP, Balgley BM, Lee CS. Electrophoresis. 2009; 30:3998–4007. [PubMed: 19960464]

2. Wang W, Sing SK, Li N, Toler MR, King KR, Nema S. Journal of Pharmaceutical Science. 2012; 431:1–11.

3. Barron AE, Blanch HW. Separation & Purification Reviews. 1995; 24:1–118.

4. Manz, A.; Pamme, N.; Iossifidis, D. Bioanalytical Chemistry. Imperial College Press; London: 2004.

5. Jorgenson JW, Lukacs KD. Science. 1983; 222:266–272. [PubMed: 6623076]

6. Swerdlow H, Dewjager KE, Brady K, Grey R, Dovichi NJ, Gesteland R. Electrophoresis. 1992; 13:475–483. [PubMed: 1451680]

7. Cohen AS, Karger BL. Journal of Chromatography. 1987; 397:409–417. [PubMed: 3654832]

8. Figeys D, Dovichi NJ. Journal of Chromatography. 1993; 645:311–317.

9. Heiger DN, Cohen AS, Karger BL. Journal of Chromatography. 1990; 516:33–48. [PubMed: 1962784]

10. Zeng Y, Harrison JD. Analytical Chemistry. 2007; 79:2289–2295. [PubMed: 17302388]

11. Malkin D, Wei B, Fogiel A, Staats SL, Wirth MJ. Analytical Chemistry. 2010; 82:2175–2177. [PubMed: 20158216]

12. Hua Y, Koshel B, Wirth MJ. Analytical Chemistry. 2010; 82:8910–8915.

13. Zeng Y, He M, Harrison DJ. Angewandte Chemie-International Edition. 2008; 47:6388–6391.

14. Cabooter D, Billen J, Terryn H, Lynen F, Sandra P, Desmet G. Journal of Chromatography A. 2008; 1178:108–117. [PubMed: 18082751]

15. Xiao DQ, Wirth M. Macromolecules. 2002; 35:2919–2925.

16. Ogston AG. Trans Faraday Soc. 1958; 54:1754–1757.

17. Ogston AG, Phelps CF. Journal of Biochemistry. 1960; 78:827–833.

18. Morris, CJOR. Protides of the biological fluid. Peeters, H., editor. Elsevier; Amsterdam: 1966. p. 543-561.

19. Rodbard D, Chrambach A. Proceedings of the National Academy of Sciences. 1970; 65:970–977.

20. Holmes DL, Stellwagen NC. Electrophoresis. 1991; 12:612–619. [PubMed: 1752240]

21. Cottet H, Garell P, Viovy JL. Electrophoresis. 1998; 19:2151–2162. [PubMed: 9761197]

22. Kopecka K, Drounin G, Slater G. Electrophoresis. 2004; 25:2177–2185. [PubMed: 15274001]

23. Giddings, JC. Unified Separation Science. John Wiley & Sons, Inc; New York: 1991.

24. Giddings JC, Kucera E, Russell CP, Myers MN. The Journal of Physical Chemistry. 1968; 72:4397–4408.

25. Tallarek U, Leinweber F, Seidel-Morgenstern A. Chemical Engineering Technology. 2002; 25:1177–1181.

26. Huang XY, Doneski LJ, Wirth MJ. Analytical Chemistry. 1998; 70:4023–4029. [PubMed: 21651239]

27. Katz, E.; Eksteen, R.; Schoenmakers, P.; Miller, N., editors. Handbook of HPLC. Marcell-Dekker, Inc; New York, NY: 1998.

28. Bird, RB.; Stewart, WE.; Lightfoot, EN., editors. Transport Phenomena. J. Wiley & Sons; New York, NY: 2007.

29. Thompson JW, Kaiser TJ, Jorgenson JW. Journal of Chromatography A. 2006; 1134:201–209. [PubMed: 16996532]

30. Khirevich S, Daneyko A, Holtzel A, Seidel-Morgenstern A, Tallarek U. Journal of Chromatography A. 2010; 1217:4713–4722. [PubMed: 20570271]

31. Narang P, Bhushan K, Bose S, Jayaram B. Physical chemistry chemical physics. 2005; 7:2364–2375. [PubMed: 19785123]

32. Svanidze AV, Koludarov IP, Lushnikov SG, Asenbaum A, Pruner C, Aliev FM, Chang CC, Kan LS. Journal of Molecular Liquids. 2012; 168:7–11.

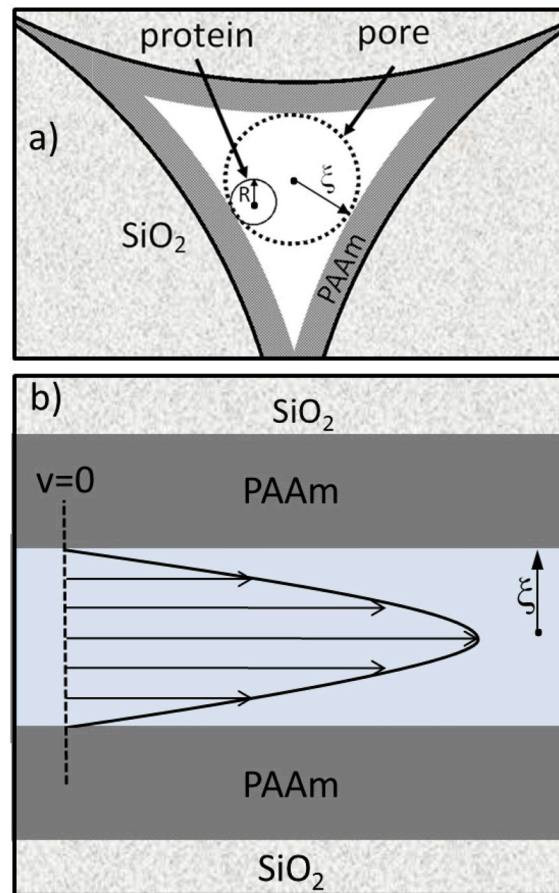33. Wei B, Malkin DS, Wirth MJ. Analytical Chemistry. 2010; 82:10216–10221. [PubMed: 21105703]

Figure 1.
a) Sketch of one cross-section of a colloidal crystal with polyacrylamide (PAAm) layer, indicating the distinction between pore radius, ξ, and protein radius, R. b) Sketch of Hagen-Poiseuille flow profile inside a small cross-section of the channel, indicating that flow goes to zero at the surface of the polyacrylamide layer.
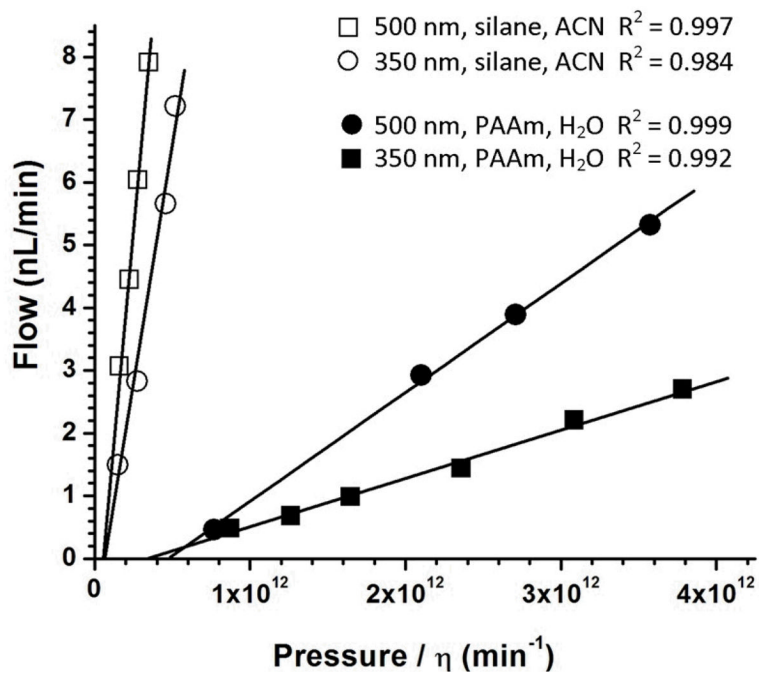
Figure 2.
Plots of flow rate vs. pressure for 2-cm long capillaries packed with 350 and 500 nm particles for different surfaces and fluids, as indicated in the figure.
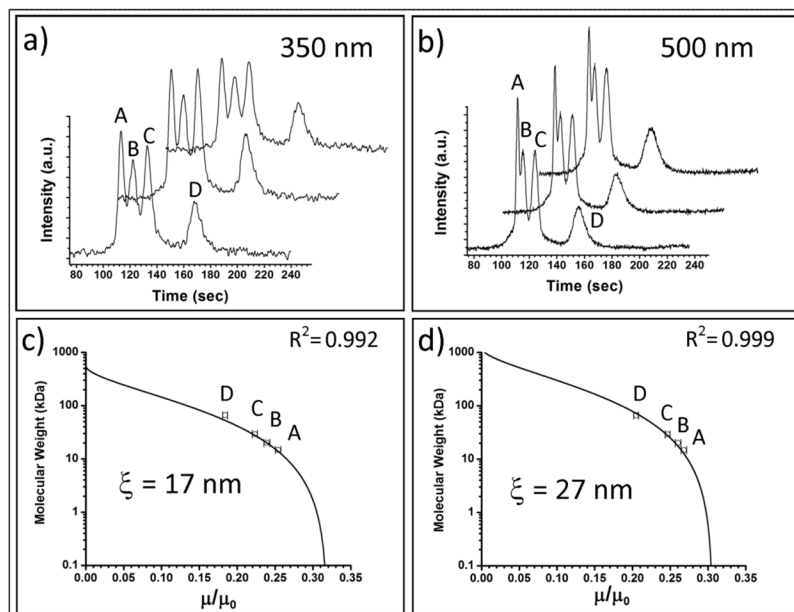
Figure 3.
Electrophoresis data run at 50 V/cm in capillaries for four proteins whose identities are listed in Table 1. Electropherograms for three replicate runs for capillaries packed with a) 350 nm particles and b) 500 nm particles. Plots of reduced mobility vs. molecular weight for c) 350 nm particles and d) 500 nm particles, where the experimental points are indicated as circles and the theoretical curves are solid.
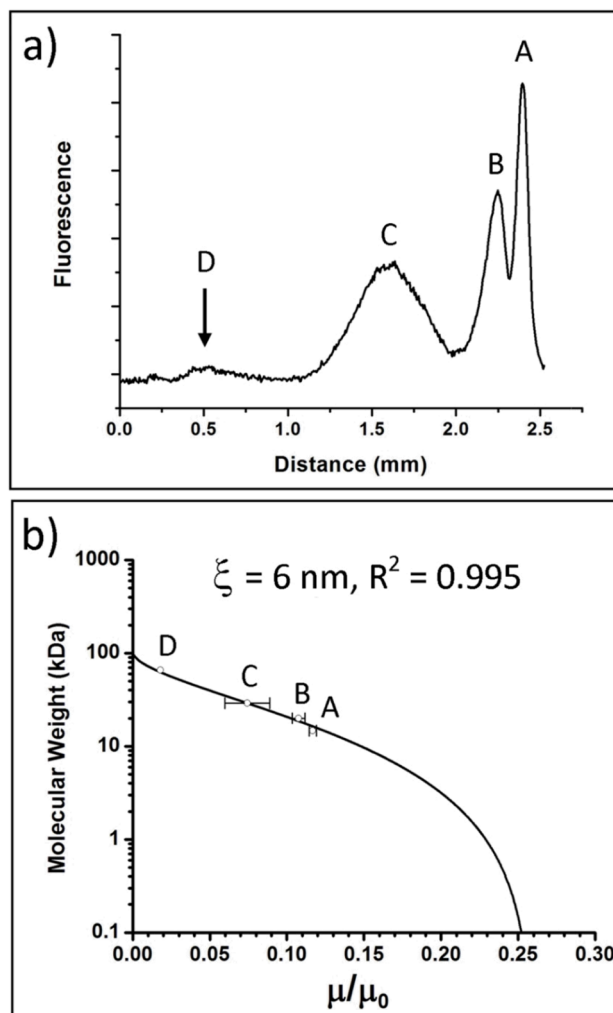
Figure 4.
Data for electrophoresis in a highly ordered colloidal crystal of 500 nm particles coated with polyacrylamide. a) Electropherogram showing all four proteins at once. b) Plot of reduced mobility vs. molecular weight. The pore radius was used as a fitting parameter with the best fit giving ξ= 6 nm.

Table 1

Summary of results for flow and electrophoresis experiments, including porosities (ε and ε$_{hyd}$), pore radius (ξ), electrophoretic mobility in an open capillary (μ$_0$), and electrophoretic mobility in the colloidal crystal (μ).

	Protein	M.W. (kDa)	Radius of gyration (nm)[c]	μ$_0$ × 10^4 (cm^{2}V^{-1}s^{-1})	Capillary 350 nm ε= 0.32 ε$_{hyd}$ =0.130 ξ = 17 nm	Capillary 500 nm ε= 0.314 ε$_{hyd}$ = 0.143 ξ = 27 nm	Channel 500 nm ε= 0.26[a] ε$_{hyd}$ = NA ξ = 6 nm[b]
					μ	μ	μ
A	Lysozyme	15	1.9	2.720 ± 0.002	0.254 ± 0.004	0.268 ± 0.006	0.113 ± 0.002
B	Trypsin Inhibitor	20	2.3	2.680 ± 0.007	0.239 ± 0.004	0.260 ± 0.004	0.104 ± 0.004
C	Carbonic anhydrase	29	2.8	2.630 ± 0.004	0.224 ± 0.003	0.246 ± 0.004	0.07 ± 0.01
D	BSA	67	4.7	2.510 ± 0.002	0.184 ± 0.003	0.205 ± 0.005	0.180[d]

[a] Estimated porosity

[b] From data fit in Figure 4b

[c] Calculated from Equation 10

[d] BSA was detectable in only one run